NASA Technical Paper 1568

Electron and Proton Absorption Calculations for a Graphite/Epoxy Composite Model

Edward R. Long, Jr.

NOVEMBER 1979

DEPARTMENT OF DEFENSE
PLASTICS TECHNICAL EVALUATION CENTER
ARRADCOM, DOVER, N. J. 07801

NASA

NASA Technical Paper 1568

Electron and Proton Absorption Calculations for a Graphite/Epoxy Composite Model

Edward R. Long, Jr.
Langley Research Center
Hampton, Virginia

National Aeronautics
and Space Administration

**Scientific and Technical
Information Branch**

1979

SUMMARY

The Bethe-Bloch stopping power relations for inelastic collisions have been used to determine the absorption of electron and proton energy for models of graphite, epoxy, and graphite/epoxy composites. Electron energies from 0.2 to 4.0 MeV and proton energies from 0.3 to 1.75 MeV, the energies that exist in geosynchronous Earth orbit (GEO), were used. Absorption profiles due to inelastic collisions for monoenergetic electrons were determined for cured neat epoxy resin, pure graphite, and graphite/epoxy composites. Electron energy losses due to bremsstrahlung were determined from these values. The absorption profiles due to inelastic collisions for monoenergetic protons were determined only for the cured epoxy resin. Finally, the dose-depth profiles in a cured epoxy resin were determined for an environment of distributed electron and proton energies that closely approximated the energy distribution in GEO.

The absorption profiles for monoenergetic particles showed that the protons did not penetrate deeper than 0.005 cm. They were absorbed at the surface of the resin, whereas the electrons, even for the lowest energy, penetrated into the bulk of the materials. Due to inelastic collisions, graphite absorbs approximately 16 percent more electron energy per unit path length than does the resin. Consequently, varying the fiber volume fraction of a structural composite between acceptable limits will not significantly alter the amount of energy the composite will absorb. Bremsstrahlung, the other mechanism by which electrons lose energy in the target materials, is not significant. Energy loss due to bremsstrahlung is less than 3 percent of the loss due to inelastic collisions.

Two important conclusions were suggested by the dose-depth profiles due to inelastic collisions in epoxy resin for electron and proton energy distributions that approximated those for GEO. First, the absorbed dose for a 10- to 30-yr mission for both electrons and protons is equal to doses which have been shown in laboratory studies to cause serious degradation of mechanical properties of composites. Second, graphite/epoxy composites are not effective shielding materials.

INTRODUCTION

Recent papers on future Earth-orbital space flight have discussed concepts for large space structures and long duration missions. These concepts inherently include two important questions: What materials should be used to build large space structures? What effects will the space environment have on properties of these materials during a long duration mission?

The choice of materials will depend significantly on the requirements for structural properties. The authors in reference 1 have stated that a high degree of stiffness will be required and that launch loads will not be important because construction of the structure will take place in space, either by modular assembly or by a structural component manufacturing technique. Powell and

S_e linear stopping power for electrons, MeV/cm

$S_{ec}(E_e)$ linear stopping power of composite for electrons having energy E_e, MeV/cm

$S_{eg}(E_e)$ linear stopping power of graphite for electrons having energy E_e, MeV/cm

S_{ei} linear stopping power for electrons due to ith type atomic centers, MeV/cm

$S_{er}(E_e)$ linear stopping power of resin for electrons having energy E_e, MeV/cm

S_p linear stopping power for protons, MeV/cm

S_{pi} linear stopping power for protons due to ith type atomic centers, MeV/cm

$S_{pr}(E_p)$ linear stopping power of resin for protons having energy E_p, MeV/cm

v particle velocity, cm/sec

v_f fiber volume fraction

x distance, cm

Z atomic number

Z_i atomic number of ith type atom

β $= v/c$

ANALYTICAL RELATIONS

Inelastic Collisions

As a charged particle passes an atomic or molecular center, it imparts an electrical pulse which excites or ionizes the center. This interaction is an inelastic collision, which is the primary means by which the charged particle loses energy. The amount of energy transferred per collision depends on the velocity of the charged particle and the distance of its closest approach. The average energy loss per unit path length through the target material may be determined for electrons and protons from expressions for the stopping power.

Electrons.- The electron linear stopping power is the average electron energy loss per unit path length due to target excitation or ionization by inelastic collision. An expression for stopping power was developed by Bethe in the early 1930's (refs. 12 and 13) and later refined (ref. 14) to the form

$$S_e = -\left(\frac{dE_e}{dx}\right)_{coll} = \frac{2Ne^4Z}{m_o v^2}\left\{\ln\left[\frac{m_o v^2 E_e}{2I^2(1-\beta^2)}\right] - \left(2\sqrt{1-\beta^2} - 1 + \beta^2\right)\ln 2 + 1 - \beta^2 + \frac{1}{8}\left(1 - \sqrt{1-\beta^2}\right)^2\right\} \quad (1)$$

where S_e has units of MeV/cm. The electron velocity is represented by $v = c\left[1 - m_o c^2/\left(E_e + m_o c^2\right)^2\right]^{1/2}$, where m_o is the electron rest mass, N is the elemental atomic density, Z is the atomic number, I is the average atomic ionization potential, e is the electron charge, E_e is the electron energy, c is the speed of light, and β is v/c. Relation (1) is for relativistic electron energies and is not applicable for electron energies less than 100 keV. Energies less than 100 keV were not important for the purpose of this paper, so the nonrelativistic expression for S_e is not included in this paper. If the target material consists of more than one element, the stopping power of the material is the sum of the atomic stopping powers, that is

$$S_e = \sum_i S_{ei} \quad (2)$$

where S_{ei} is for the ith type atom. Simple addition is justified by the additivity rule of Bragg (ref. 11).

Protons.- An expression for proton energy loss per unit path length in a material, proton linear stopping power S_p, was also developed by Bethe (refs. 12 and 13). The expression is similar to that for electrons,

$$S_p = -\frac{dE_p}{dx} = \frac{4e^4}{m_o v^2} NZ\left\{\ln\left[\frac{2m_o v^2}{I(1-\beta^2)}\right] - \beta^2\right\} \quad (3)$$

where S_p is in MeV/cm. The linear stopping power for protons S_p is an average energy loss as it is for electrons. Relation (3) is for relativistic proton velocities and is not applicable for proton energies less than 100 keV. If the target material consists of more than one type of elemental center, then

$$S_p = \sum_i S_{pi} \quad (4)$$

where S_{pi} is the linear stopping power for the ith type center.

Bremsstrahlung

Energy loss from energetic electrons in the form of bremsstrahlung becomes significant for electron energies greater than 10 to 100 MeV. The energy value above which significant bremsstrahlung losses occur depends on the target material. Bremsstrahlung is based on the classical theory that charged particles passing at high speed close to the nucleus of an atom will decelerate and radiate electromagnetic energy in the form of gamma radiation and X-radiation. The amount of electron energy loss due to bremsstrahlung may be compared to inelastic losses (ref. 15) by the relation

$$\frac{S_b}{S_e} = \frac{E_e Z}{819 \text{ MeV}} \tag{5}$$

MATERIAL MODEL

Neat Resin

The resin selected for modeling was tetraglycidyl 4,4' diamino diphenyl methane (TG 4,4' DDM) epoxy cured with diamino diphenyl sulfone (DDS). Figure 1 is a depiction of the epoxy model. The dashed line encloses the repeat cured unit. The technique of selecting a repeat unit for modeling of molecular structures has been previously used in the determinations of S_e and S_p for much simpler polymer systems (ref. 11). The model is given the name CNOSH1, where the letters represent the atomic constituents and the number represents the number of TG 4,4' DDM molecules in each repeat unit. Table I contains the values of the atomic parameters for CNOSH1 that are required for using the equations presented in the preceding section. The stopping powers for each type of atomic center were determined and the results were added for each electron and proton energy. The sums, $S_{er}(E_e)$ and $S_{pr}(E_p)$, are the electron and proton linear stopping powers of the resin model.

Graphite Fibers

The electron stopping power of graphite fibers was determined from the stopping power of carbon. The carbon parameters were the same as given for carbon in table I except the value of N was 9.036×10^{22} atoms/cm^3. The results, $S_{eg}(E_e)$, were used as the stopping power of graphite.

Graphite/Epoxy Composite

Electron stopping power of the composite was determined from the relation $S_{ec}(E_e) = v_f S_{eg}(E_e) + (1 - v_f) S_{er}(E_e)$ where v_f is the composite fiber volume fraction. This equation expresses the combined electron stopping power of resin and fiber, with each value weighted for its volume content, as a weighted average of energy absorption of the composite.

RESULTS AND DISCUSSION

Electron Inelastic Collisions

Resin.- The electron stopping power for CNOSH1 is plotted in figure 2 for several electron energies. Stopping power curves included in figure 2 are from data in reference 11 for three other polymer systems. The values of stopping power for these three simpler systems were also calculated with the Bethe-Bloch equation. The stopping power for CNOSH1 is highest because the density of the epoxy was 1.32 g/cm^3, whereas the densities used for polyethylene, polystyrene, and polyvinyl chloride were 0.95, 1.02, and 1.25 g/cm^3, respectively. As demonstrated in figure 2, the epoxy is much more effective for absorbing electron radiation, hence a better radiation shield, than the other materials. The mass stopping powers, obtained by normalizing the stopping powers in figure 2 with respect to their polymer masses, would be nearly the same for all four compounds. Moreover, the mass stopping power of CNOSH1 is similar to those tabulated in reference 10 for oxygen, iron, and aluminum. Indeed, the stopping powers for any material may be estimated by multiplying the mass stopping power of any standard, such as aluminum, by the density of the material in question. Aluminum, because of its higher density, is a more effective shield than is epoxy. However, a trade-off must be made between shielding effectiveness and other properties, such as weight and stiffness, when deciding which material to use. The stopping powers for CNOSH1 and aluminum are plotted in figure 3 to compare the shielding provided by the two materials.

Figure 4 is a plot, in terms of path length, of electron stopping power in CNOSH1 for several initial electron energies from 0.2 to 4.0 MeV. These energies are typical of most electrons in the space environment. The energy loss per unit path length is nearly constant along the initial portion of the path for electrons with initial energies greater than 0.5 MeV. The length of path for constant energy loss depends on the initial energy of the electron. The loss rate increases rapidly for approximately the last 0.2 cm of path length, regardless of the initial energy. Calculations of electron energy loss were not made for remaining electron energies of less than 0.1 MeV because relation (1) is not applicable for energies less than 100 keV and because the remaining 100 keV does not appreciably alter the estimate of path length.

Total path length of an electron is defined in this paper as the travel distance required to lose all but 0.1 MeV of energy and is plotted as a function of initial electron energy in figure 5. The data points have a straight-line fit:

$$\text{Path length (resin)} = -0.04 + 0.41E_{eo} \qquad (6)$$

where path length is in cm and initial electron energy E_{eo} is in MeV. The depth of penetration (practical mean free path) is approximately eight-tenths of the path length (refs. 11 and 15). Therefore, the depth of penetration for which uniform energy loss occurs is determined by subtracting 0.2 cm from relation (6) and then multiplying the difference by 0.8. The amount 0.2 cm is sub-

tracted because the absorption for approximately the last 0.2 cm of total path length is nonuniform. Hence, the penetration of an electron for which the absorption of energy is approximately uniform is

$$P_{eu}\ (\text{resin}) = 0.8(-0.24 + 0.41E_{eo}) \tag{7}$$

The shape of the energy loss curves for electrons (fig. 4) and relations (6) and (7) may be applied for an actual TG 4,4' DDM epoxy cured with DDS, because the carbon centers dominate the energy loss process. The ratio of the number of carbon centers to the total number of atomic centers in CNOSH1 and in the actual epoxy are not significantly different. For example, the ratio is 0.41 for CNOSH1 and 0.39 for CNOSH1000.

Graphite.- Figure 6 is a plot of electron energy loss in graphite for distance along the path length. The initial electron energies are the same as shown in figure 4. The uniform energy loss is 3.0 MeV/cm. The uniform loss per unit path length in graphite is approximately 16 percent higher than in the resin model. The total path length for an electron with an initial energy of 4.0 MeV is 1.3 cm, which is 18 percent shorter than the path length in the resin model. This path-length difference is more significant for lower initial electron energies. In graphite for example, the total path length of electrons with initial energy of 0.2 MeV is 0.3 cm, or 40 percent less than the total path length in the resin model.

The total path-length data from figure 6 is plotted in figure 7 as a function of initial electron energy. The data have a straight-line fit, with

$$\text{Path length (graphite)} = -0.04 + 0.33E_{eo} \tag{8}$$

where path length is in cm and E_{eo} is in MeV. A relation for penetration with uniform energy loss is found in the manner discussed for the resin model:

$$P_{eu}\ (\text{graphite}) = 0.8(-0.24 + 0.33E_{eo}) \tag{9}$$

Composite.- Figure 8 is a plot of electron energy losses in the resin, graphite, and composite models for a fiber volume fraction v_f of 0.62 and an electron with an initial energy of 4.0 MeV. The value of 0.62 was chosen because this value corresponds to the typical v_f for graphite/epoxy prepreg and, therefore, v_f for a composite would be at least this large. The uniform energy loss for $v_f = 0.62$ is approximately 12 percent greater than for neat resin, and total path length for $v_f = 0.62$ is 14 percent less than for neat resin. The total path-length data in figure 8 can also be used to determine the total penetration of electrons in a composite. Figure 9 is a plot of the total path-length data as a function of v_f for 4.0 MeV electrons. The data have a straight-line fit when

$$\text{Path length (composite)} = 1.59 - 0.29v_f$$

A more general expression for path length may be found from relations (6) and (8):

$$\text{Path length (composite)} = -0.04 + (0.41 - 0.08v_f)E_{eo} \tag{10}$$

The penetration for an electron with uniform energy loss from relations (7) and (9), is

$$P_{eu}\ \text{(composite)} = 0.8\left[-0.24 + (0.41 - 0.08v_f)E_{eo}\right] \tag{11}$$

Relation (11) may be used to determine the radiation shielding graphite/epoxy composite would provide. Given in table II are the minimum energies required for normally incident electrons to pass through different thickness composites with $v_f = 0.62$. The trapped electron spectra shown in figure 10 are for selected orbits (ref. 8, p. 47). Comparison of data in table II and figure 10 suggests that a majority of the electrons in any orbital environment will pass through composites of the thicknesses tabulated.

Proton Inelastic Collisions

Resin.- Figure 11 is a plot of proton energy absorption as a function of path length in CNOSH1 for several initial proton energies from 0.31 to 1.74 MeV. This energy is typical of that found in space (ref. 8). Because protons are not appreciably deflected, path length and penetration are approximately the same. The calculations were not made for energies less than 0.1 MeV because relation (3) is not appropriate for proton energies less than 0.1 MeV. The immediate observation from figure 11 is that proton absorption occurs at the surface. Figure 12 is a plot of proton penetration in CNOSH1 as a function of initial proton energy. The data have a power curve fit of

$$P_p = 1.84(10)^{-3}E_{po}^{1.59}$$

where P_p is in cm and E_{po} is in MeV. The data for proton penetration in CNOSH1 would be expected to be similar to that in TG 4,4' DDM cured with DDS because of the same reasons given in the discussion of electron energy loss in resins.

Graphite and composites.- Because proton energy typical of the orbital environment is absorbed at the surface of resins, the proton absorption will also be at the surface of graphite and composites. If the composite has a resin-rich surface, the proton radiation would probably not reach the fibers.

Different composite values of v_f would not affect the proton absorption profile in the composite.

Bremsstrahlung

Resin.- The loss in energy due to bremsstrahlung is applied only for electrons. For protons with E_p = 1.75 MeV, no significant energy loss occurs through bremsstrahlung. Relation (5) is used to determine the ratio of loss due to bremsstrahlung to loss due to inelastic collisions. For the resin,

$$S_b = \sum_i S_{bi} = \frac{E_e}{1.31 \times 10^{-3}} \sum_i S_{ei} Z_i$$

where the summation is over the different atomic types. The ratios S_b/S_e for CNOSH1 are plotted in figure 13 for several electron energies up to and including 20 MeV. At 4.0 MeV, the amount of electron energy loss in CNOSH1 due to bremsstrahlung is 3.0 percent of the loss due to inelastic collisions. Of course if higher energy electrons are used to simulate space radiation of composites, bremsstrahlung may become a significant factor. The ratios would not be expected to differ appreciably for TG 4,4' DDM cured with DDS, because the carbon atoms dominate the absorption of electron energy. Indeed, if the ratios S_b/S_e for CNOSH1 are substituted into relation (5), the effective atomic number is 6.1.

Graphite and composite.- The atomic number Z for graphite is 6.0. The ratio of S_b/S_e for $Z = 6.0$ and electron energies up to and including 20.0 MeV is almost identical to the ratios for the resin model CNOSH1 shown in figure 13.

The percentage of electron energy loss in a graphite/epoxy composite due to bremsstrahlung is almost identical to that of the resin, since the value of Z for graphite, 6.0, and the effective value of Z for CNOSH1, 6.1, are approximately the same. Therefore, electron energy losses due to bremsstrahlung will not vary appreciably with v_f.

Absorption and Penetration of Particulate Radiation in Epoxy for Geosynchronous Earth Orbit

The plans for potential long duration flight of large space structures have frequently cited GEO as the orbit necessary for accomplishing mission goals. For the mission to be successful, the structure and the subsystems within must be capable of withstanding the total radiation dose. Therefore, designers must know what dose will be absorbed by the structure and how much radiation energy will pass through the structure. The absorbed dose and the amount of energy transmitted are presented in this section for epoxy resin in a GEO environment.

Calculations are not included for graphite and graphite/epoxy composites because, as was discussed in the preceding section, the path length and linear energy absorption of electrons for these materials do not differ appreciably from those for the resin. The calculations of absorption and transmission were made using equations (1) and (3) and the data for distribution of particle energy given in reference 8 (pp. 37-62).

Electrons.- The amount of electron energy calculated to be absorbed and transmitted by cured epoxy resin in GEO is shown in figure 14. The calculations did not include the last 100 keV of energy for each electron. The epoxy is the same model as described earlier. For reference, the nominal thicknesses of 4- and 8-ply composites are included in the figure. The large amount of absorption near the surface occurs because of the large number of lower energy electrons. Thus, a cured resin would experience a higher dose in the front portion of its bulk and no dose in its final portion if it were sufficiently thick. In figure 14, the dose rate at the front surface is approximately 2.2×10^3 rads/hr and at 0.04 cm the dose rate is 2.7×10^3 rads/hr. After 30 years, the absorbed doses at these two depths are 5.8×10^8 and 7.2×10^8 rads. These are the doses discussed in the introduction for which polymer materials began to show serious mechanical property deterioration in the laboratory. These values could easily be doubled by the radiation a large space structure would experience during the 6 to 12 months required for transition from low Earth orbit to GEO. Consequently, the total dose at some intermediate period of a long duration mission could cause serious structural failure. However, other failures may precede structural failures simply because of the electron radiation that may be transmitted by a composite.

Energy transmitted through a structural wall and into the interior of a spacecraft may degrade the subsystems within the spacecraft. The amount of transmitted energy may be substantially high as shown in the dose-depth profile (fig. 14). Thicknesses of resin equivalent to 4- and 8-ply composites would transmit approximately 70 and 40 percent, respectively, of the incident radiation. These values would be approximately 15 percent less for a composite because of the higher absorption of the graphite content. But still, the amount of transmitted radiation would be sufficient to damage interior electrical and optical systems. For example, glass will deteriorate at doses as low as 10^5 rads (ref. 8, pp. 403-431). Consequently, thin graphite/epoxy composites are not good shields to electron radiation.

Protons.- Graphite/epoxy composites will, however, provide shielding for proton radiation. The dose-depth profile for the cured epoxy resin in a GEO proton environment is shown in figure 15. The last 100 keV of energy for each proton is not included in the profile. The proton energy is absorbed in approximately 0.005 cm, a thickness equal to one-tenth of a composite ply. After 30 years, the total dose at the surface would be 10^{10} rads which, based on the laboratory studies discussed earlier, may seriously reduce the stiffness of graphite/epoxy. The extremely large surface dose suggests that problems may occur even if a protective thermal coating were used. Generally, these coatings are thin, hence proton energy would be absorbed at the interface of the coating and the composite. At doses as high as 10^{10} rads, the interface could rupture and lead to removal of the coating as well as deterioration of the optical properties of the coating.

CONCLUDING REMARKS

The Bethe-Bloch stopping power relations for inelastic collisions have been used for cured epoxy and graphite to determine their absorption of energy from electron and proton space radiation. The calculations were made for monoenergetic particles and for the energy distribution which exists in geosynchronous Earth orbit.

The results for monoenergetic particles show that proton energy is absorbed near the surface, whereas electrons penetrate and their energies are absorbed in the bulk of the material. The absorption of electron energy in pure graphite is only 16 percent higher than in cured neat resin. Therefore, absorption of energy will not vary appreciably for the practical range of fiber content in structural graphite/epoxy composites. Electron energy losses due to bremsstrahlung, which were determined from the losses due to inelastic collisions, were less than 3 percent of the total energy loss for energy values which occur in space. Therefore, bremsstrahlung is not an important process for graphite/epoxy composites in space.

The results for energy distributions for electron and proton radiation in geosynchronous Earth orbit (GEO) suggests that minimum dose levels of 7.2×10^8 rads for electrons and 10^{10} rads for protons may occur for a 30-yr mission. Laboratory studies have shown that these dose values will cause serious deterioration of mechanical properties of graphite/epoxy composites. For electron radiation in GEO, a significant portion of radiation energy would pass through even an 8-ply composite and thus could damage electrical and optical systems within a spacecraft structure. For proton radiation in GEO, the dose profile suggests that thin coatings for thermal control could degrade and rupture due to energy absorption at the interface of the coating and the composite.

Langley Research Center
National Aeronautics and Space Administration
Hampton, VA 23665
October 10, 1979

REFERENCES

1. Hedgepeth, John M.; Mikulas, Martin M., Jr.; and MacNeal, Richard H.: Practical Design of Low-Cost Large Space Structures. Astronaut. & Aeronaut., vol. 16, no. 10, Oct. 1978, pp. 30-34.

2. Powell, Denis J.; and Browning, Lee: Automated Fabrication of Large Space Structures. Astronaut. & Aeronaut., vol. 16, no. 10, Oct. 1978, pp. 24-29.

3. Goodwin, Charles J.: Space Platforms for Building Large Space Structures. Astronaut. & Aeronaut., vol. 16, no. 10, Oct. 1978, pp. 44-47.

4. Card, Michael F.; Kruszewski, Edwin T.; and Guastaferro, Angelo: Technology Assessment and Outlook. Astronaut. & Aeronaut., vol. 16, no. 10, Oct. 1978, pp. 48-54.

5. Paillous, A.: Mechanisms of Radiation Damage in Polymers. ONERA Paper presented at International Seminar on Simulation and Space (Toulouse, France), Sept. 10-14, 1973.

6. Evans, D.; Morgan, J. T.; Sheldon, R.; and Stapleton, G. B.: Post Irradiation Mechanical Properties of Epoxy Resin/Glass Composites. RHEL/R-200, Sci. Res. Counc. (British), June 1970.

7. Von Bassewitz, H.: Behaviour of Carbon Fibre Composites Under Simulated Space Environment. Proceedings International Conference on Evaluation of the Effect of the Space Environment on Materials (Toulouse, France), June 17-21, 1974, pp. 525-537.

8. Rittenhouse, John B.; and Singletary, John B.: Space Materials Handbook - Third Edition. NASA SP-3051, 1969. (Also available as AMFL-TR-68-205.)

9. Bekey, Ivan: Big Comsats for Big Jobs at Low User Cost. Astronaut. & Aeronaut., vol. 17, no. 2, Feb. 1979, pp. 42-56.

10. Berger, Martin J.; and Seltzer, Stephen M.: Tables of Energy Losses and Ranges of Electrons and Positrons. NASA SP-3012, 1964.

11. Makhlis, P. A. (Israel Program for Scientific Translations, transl.): Radiation Physics and Chemistry of Polymers. John Wiley & Sons, [1975].

12. Bethe, H.: Quantenmechanik der Ein- und Zwei-Elektronenprobleme. Handb. Phys., Bd. XXIV, Kap. 3, Julius Springer (Berlin), 1933, pp. 273-560.

13. Bethe, H.: Zur Theorie des Durchgahgs schneller Korpus-kularstrahlen durch Materie. Ann. Physik, vol. 5, no. 3, June 10, 1930, pp. 325-400.

14. Bethe, Hans A.; and Ashkin, Julius: Passage of Radiations Through Matter. Experimental Nuclear Physics, Volume I, E. Segrè, ed., John Wiley & Sons, Inc., c.1953, pp. 166-357.

15. Spinks, J. W. T.; and Woods, R. J.: An Introduction to Radiation Chemistry. John Wiley & Sons, Inc., c.1964.

TABLE I.- VALUES OF ATOMIC PARAMETERS FOR CNOSH1

Parameters	Carbon	Nitrogen	Oxygen	Sulfur	Hydrogen
Atom density, N, 10^{22} atoms/cm^3	4.3294	0.4810	0.7216	0.1203	5.0509
Atomic number, Z	6	7	8	16	1
Ionization potential, I, 10^{-4} MeV	.78	.88	1.01	1.54	1.80

TABLE II.- MINIMUM ENERGY REQUIRED FOR ELECTRONS TO PASS THROUGH COMPOSITES[a]

Thickness, cm (number of plies)	Minimum energy, MeV
0.025 (2)	0.21
.050 (4)	.30
.075 (6)	.40
.100 (8)	.49

[a]Fiber volume fraction, $v_f = 0.62$.

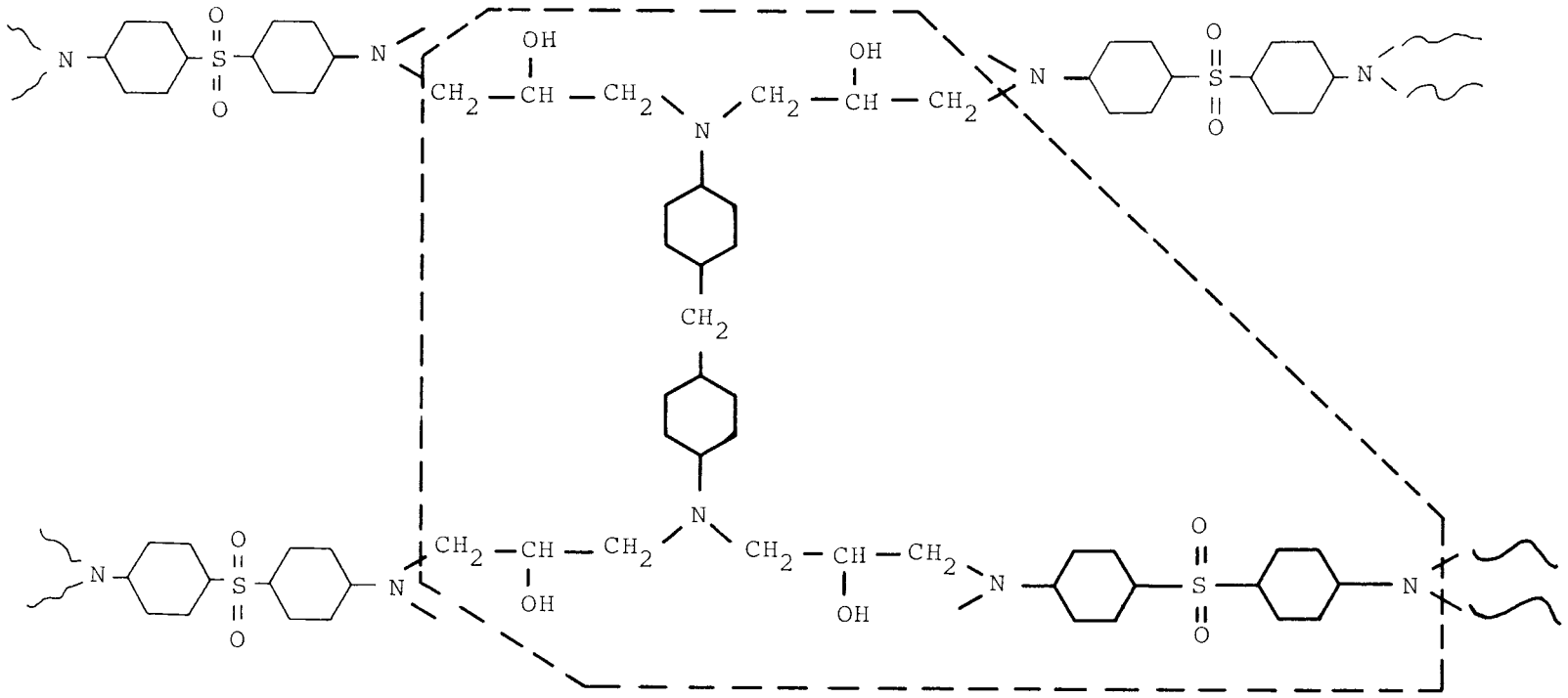

Figure 1.- Model, CNOSH1, of tetraglycidyl 4,4' diamino diphenyl methane epoxy cured with diamino diphenyl sulfone.

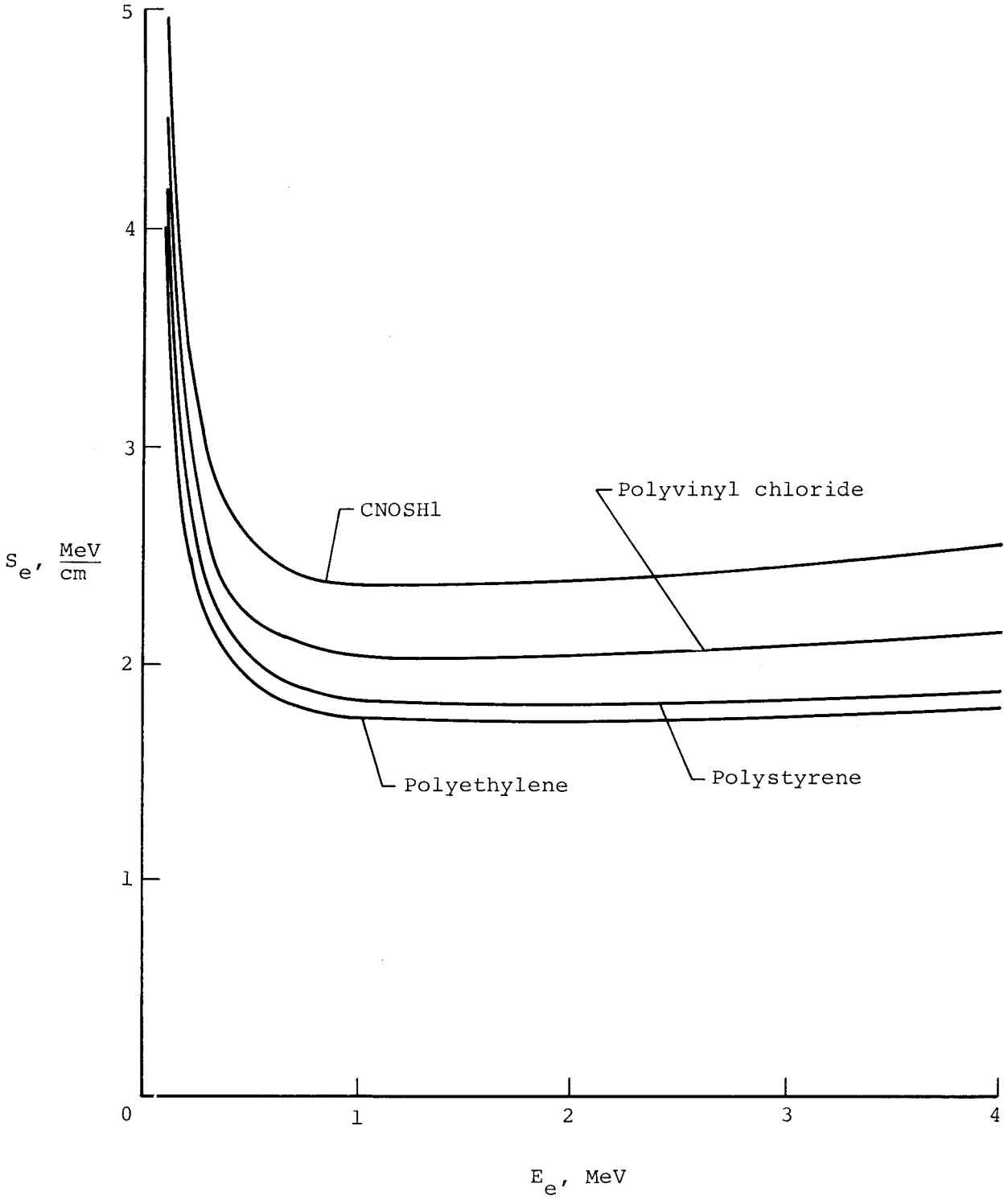

Figure 2.- Electron stopping powers for CNOSH1 and several other polymer systems.

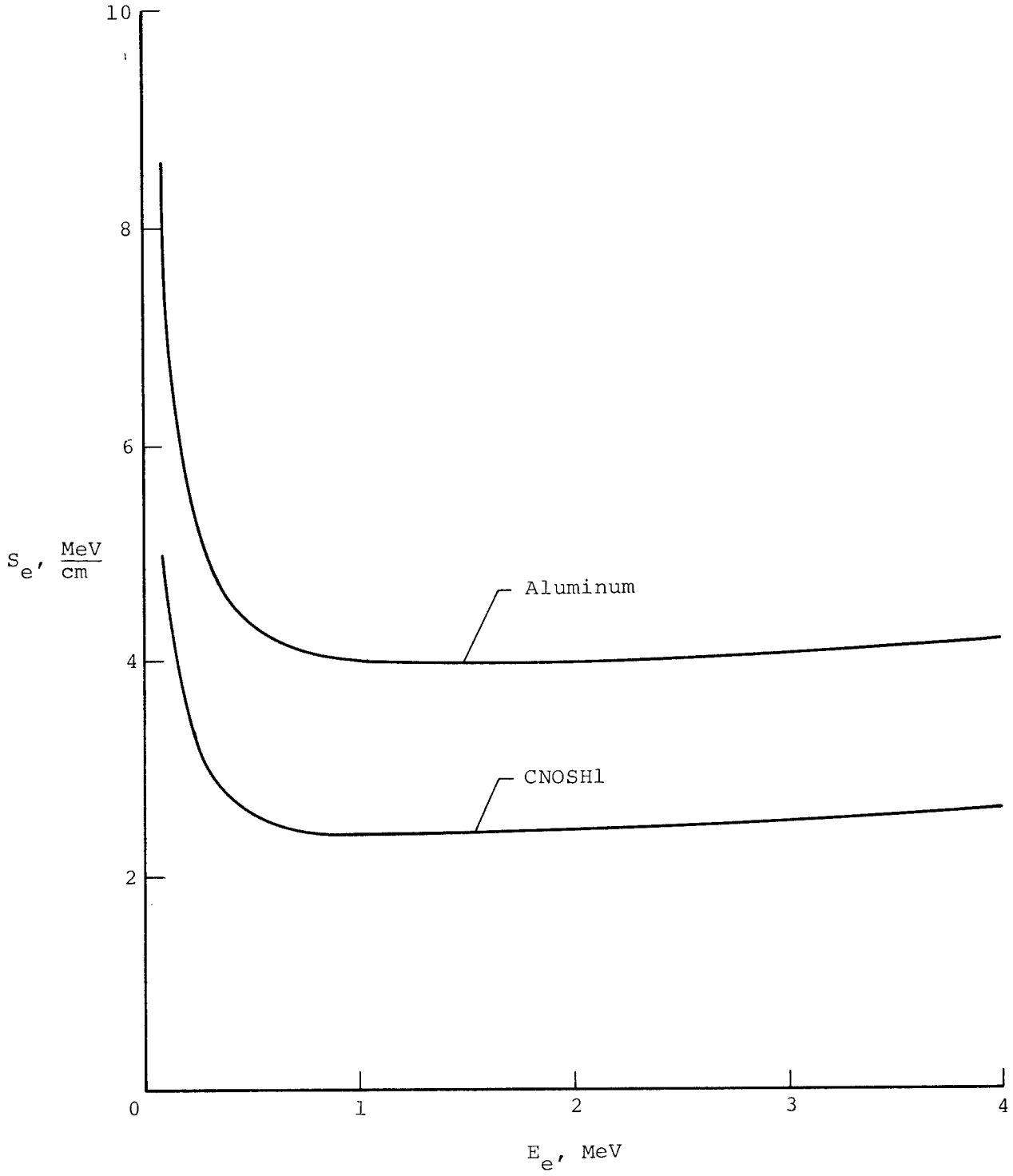

Figure 3.- Electron stopping power for CNOSH1 and aluminum.

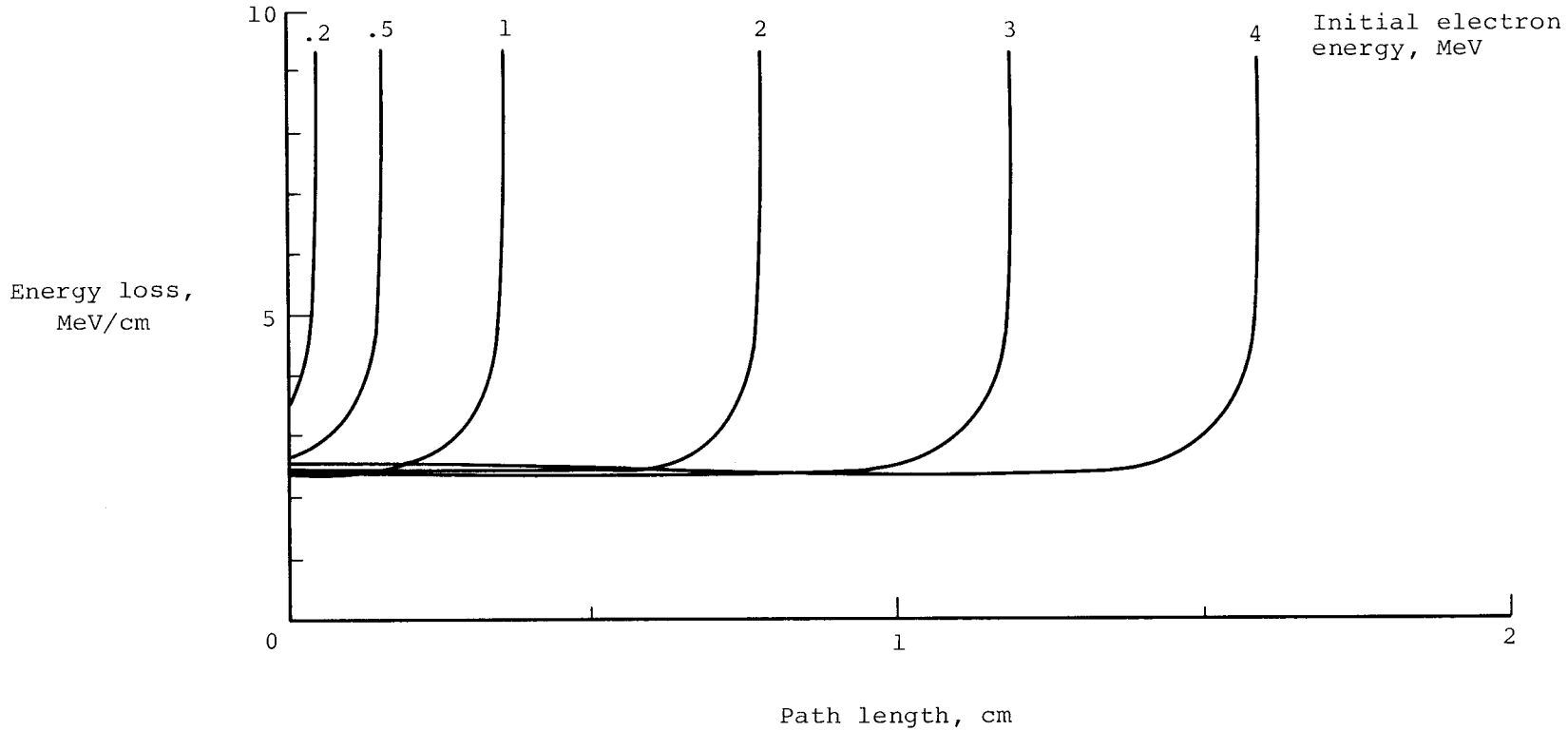

Figure 4.- Loss of electron energy in CNOSH1 epoxy resin model.

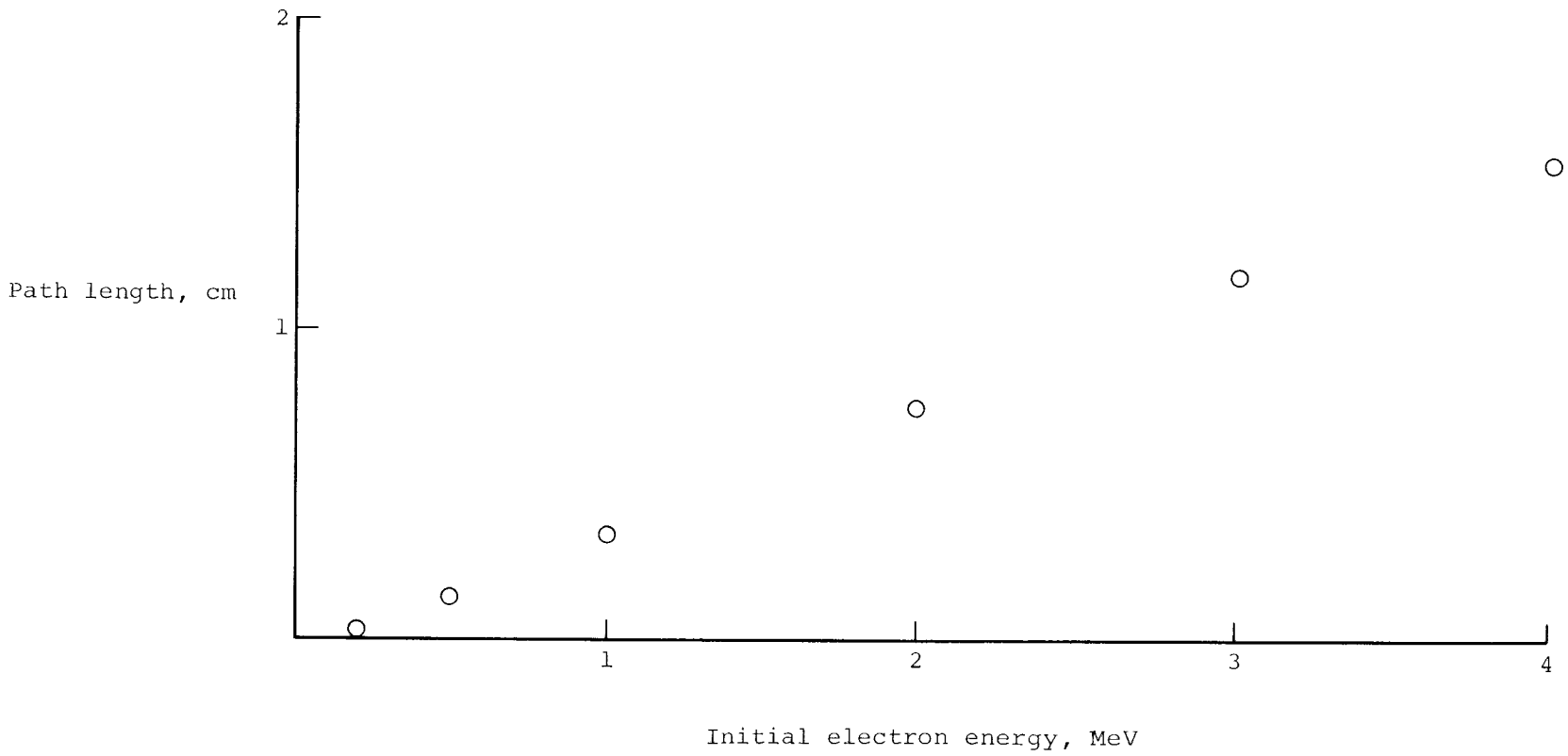

Figure 5.- Electron path length in CNOSH1 resin model as function of initial electron energy.

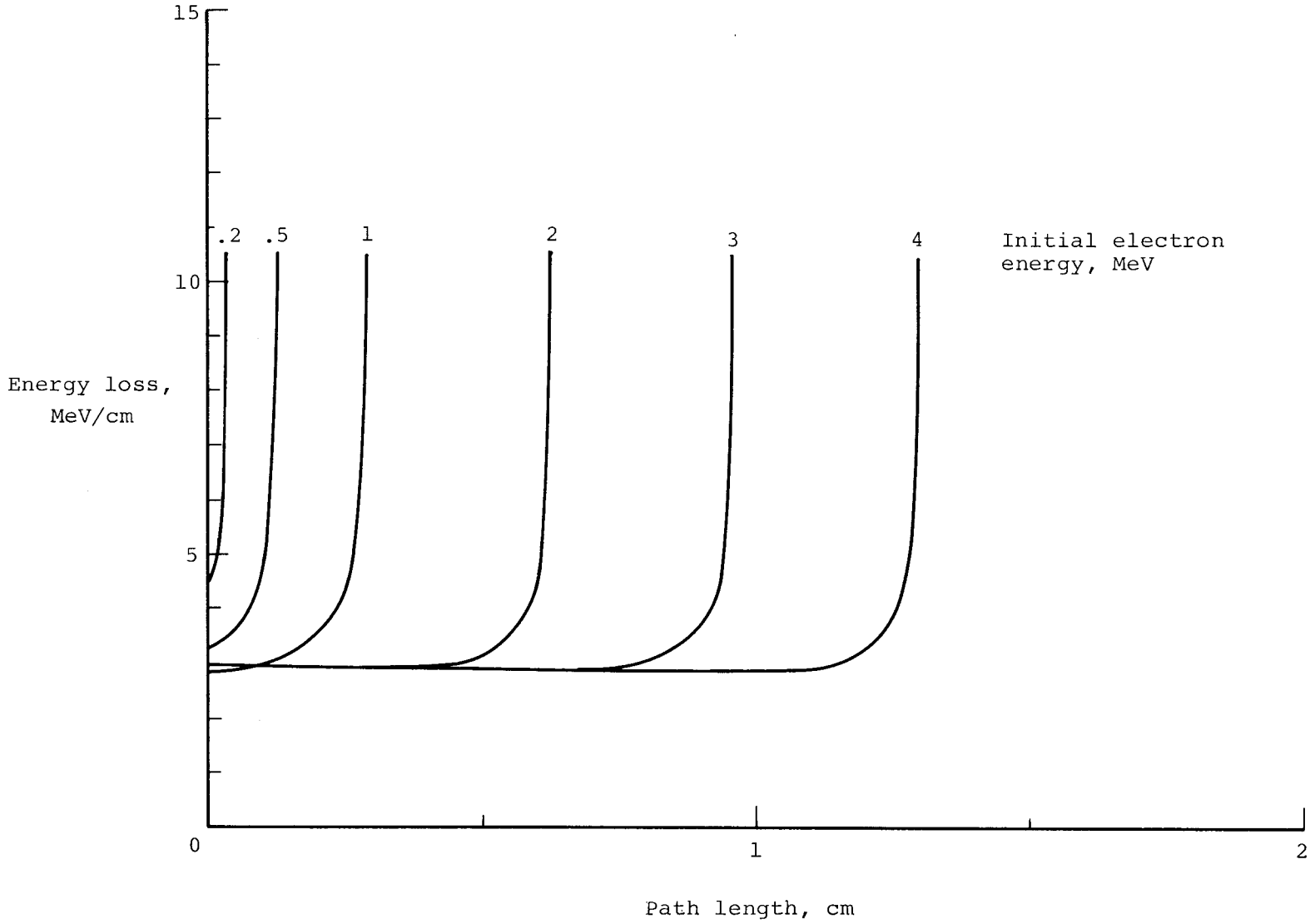

Figure 6.- Loss of electron energy in graphite model.

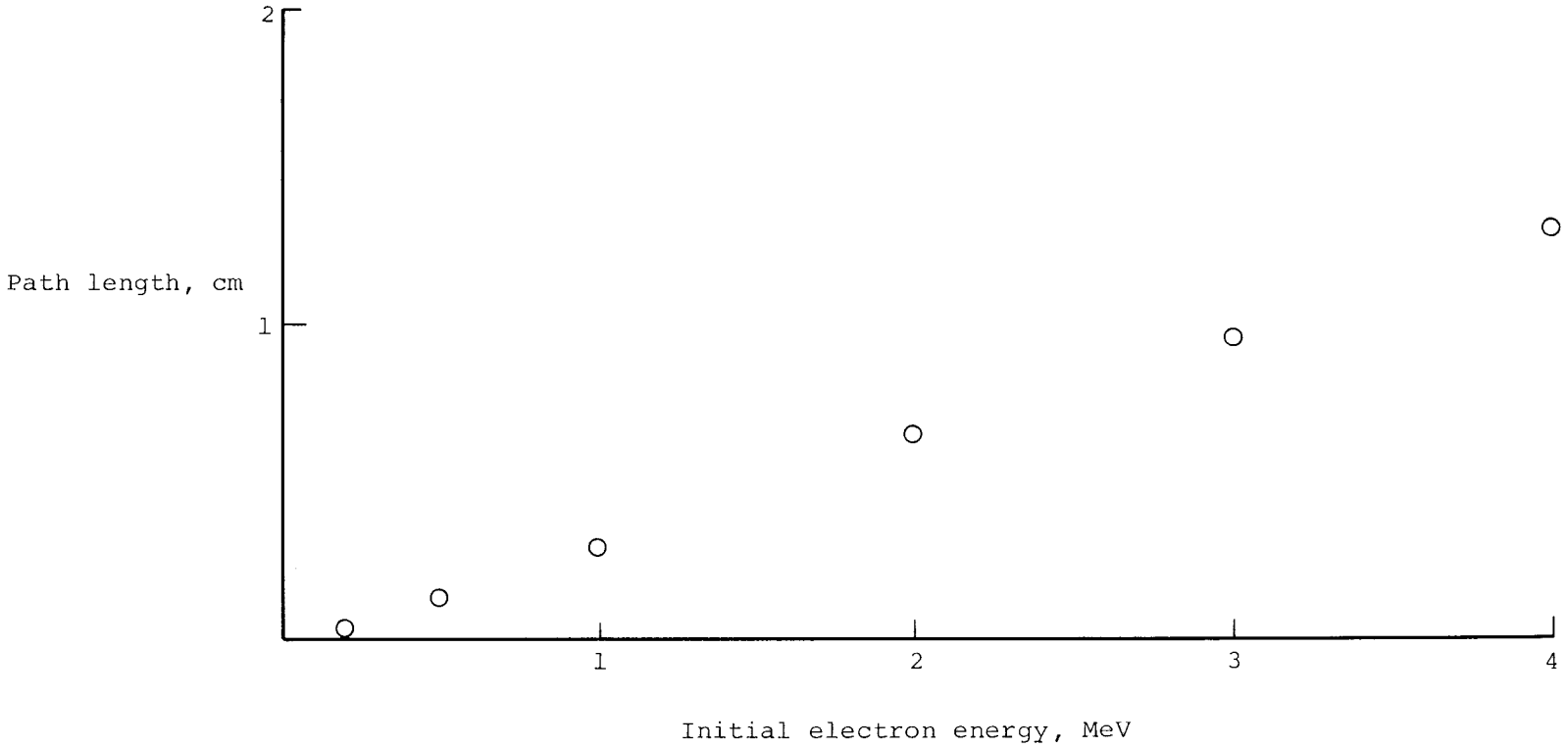

Figure 7.- Electron path length in graphite model as function of initial electron energy.

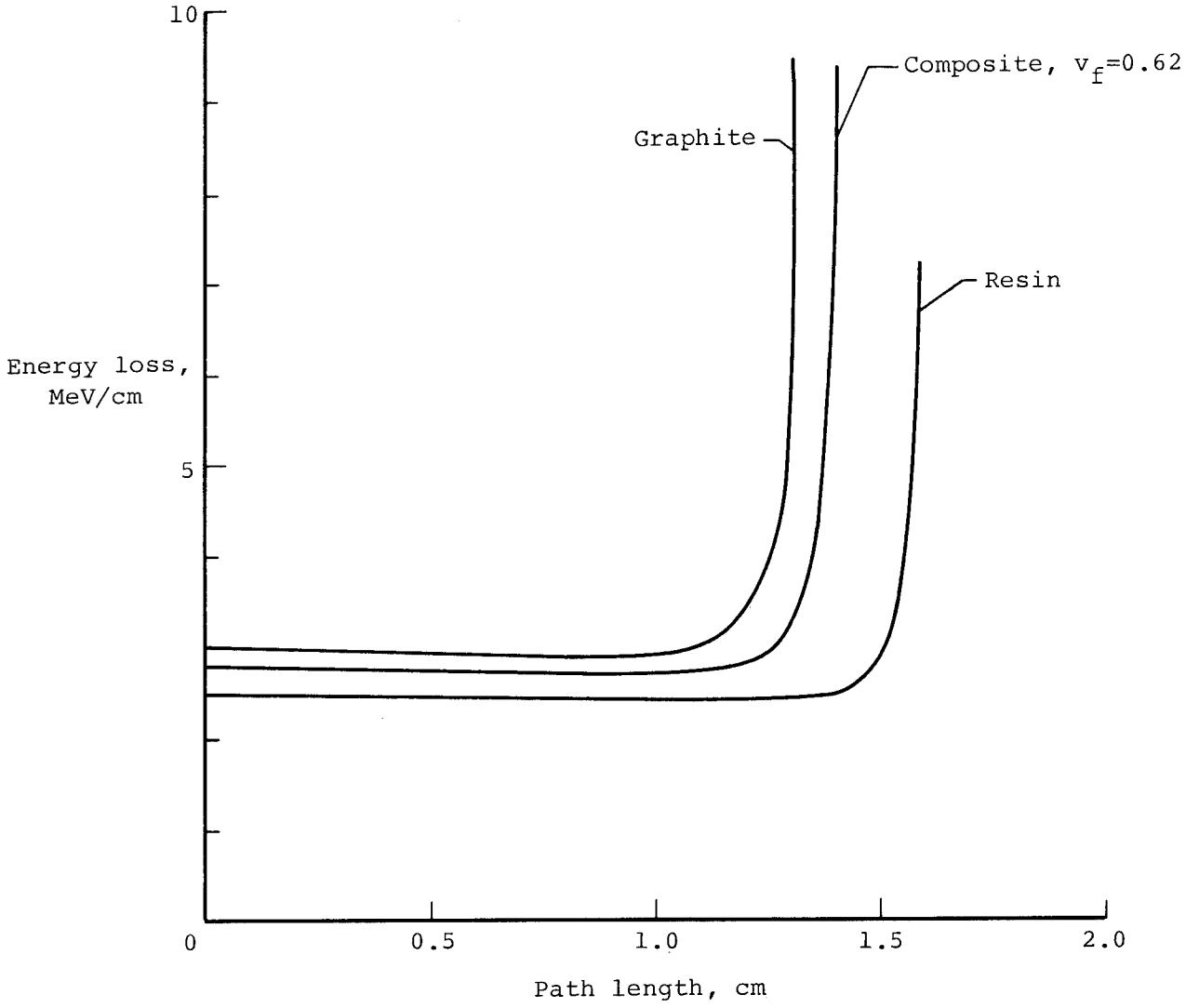

Figure 8.- Energy loss of 4.0 MeV electrons in resin, graphite, and composite models.

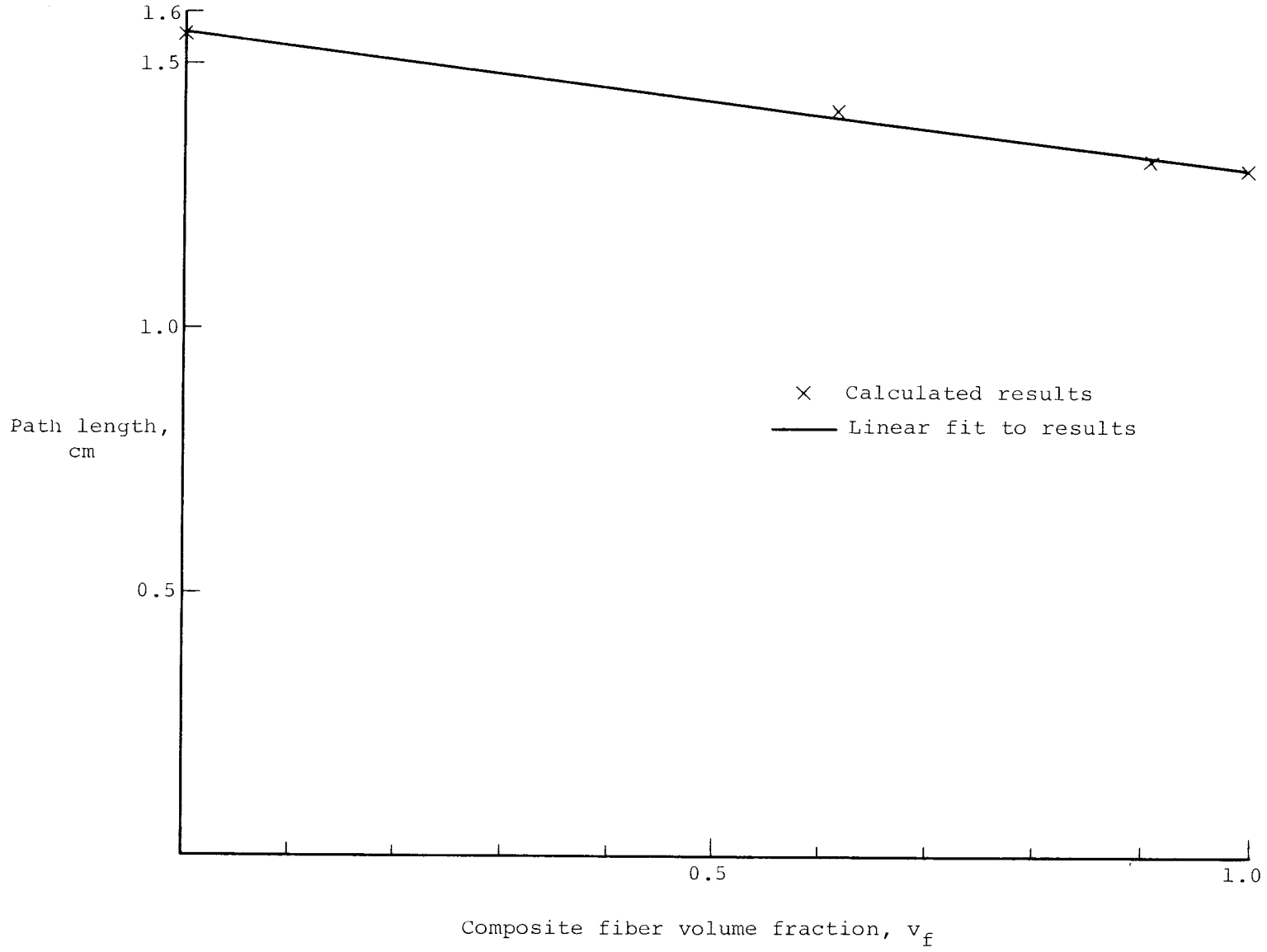

Figure 9.- Path length of 4.0 MeV electrons in graphite/epoxy model.

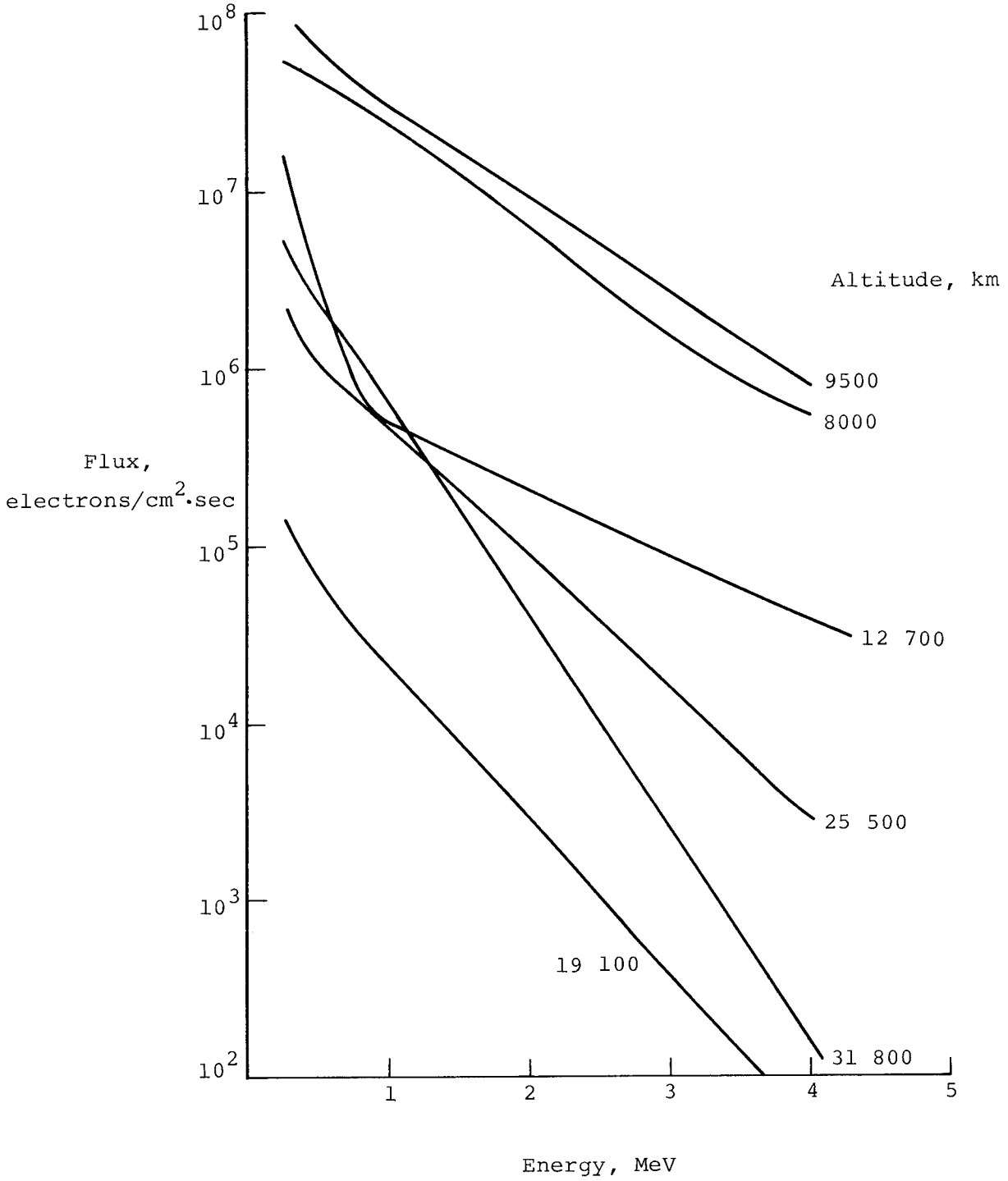

Figure 10.- Trapped electron spectra in Earth orbital environment.

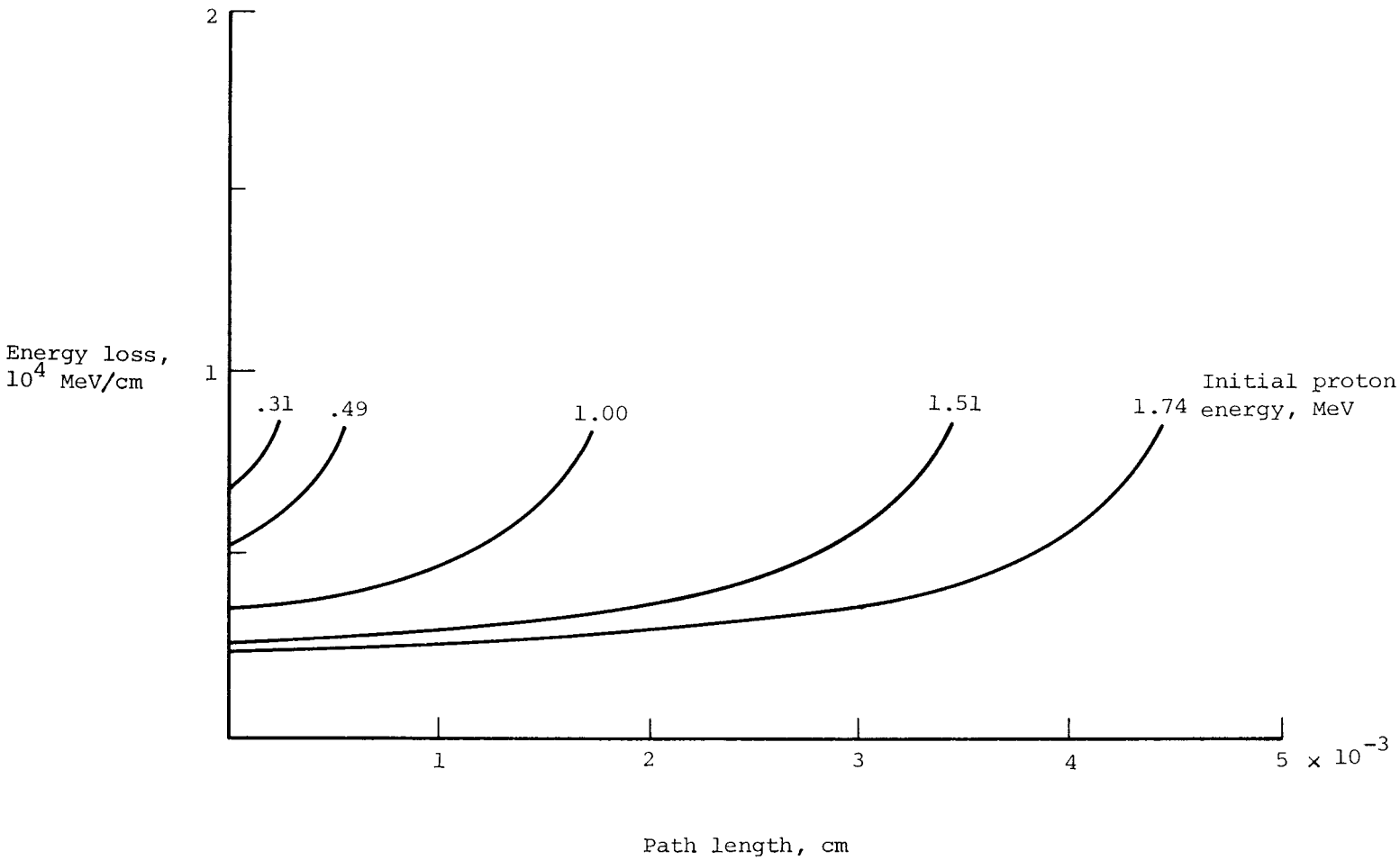

Figure 11.- Proton energy absorption in CNOSH1.

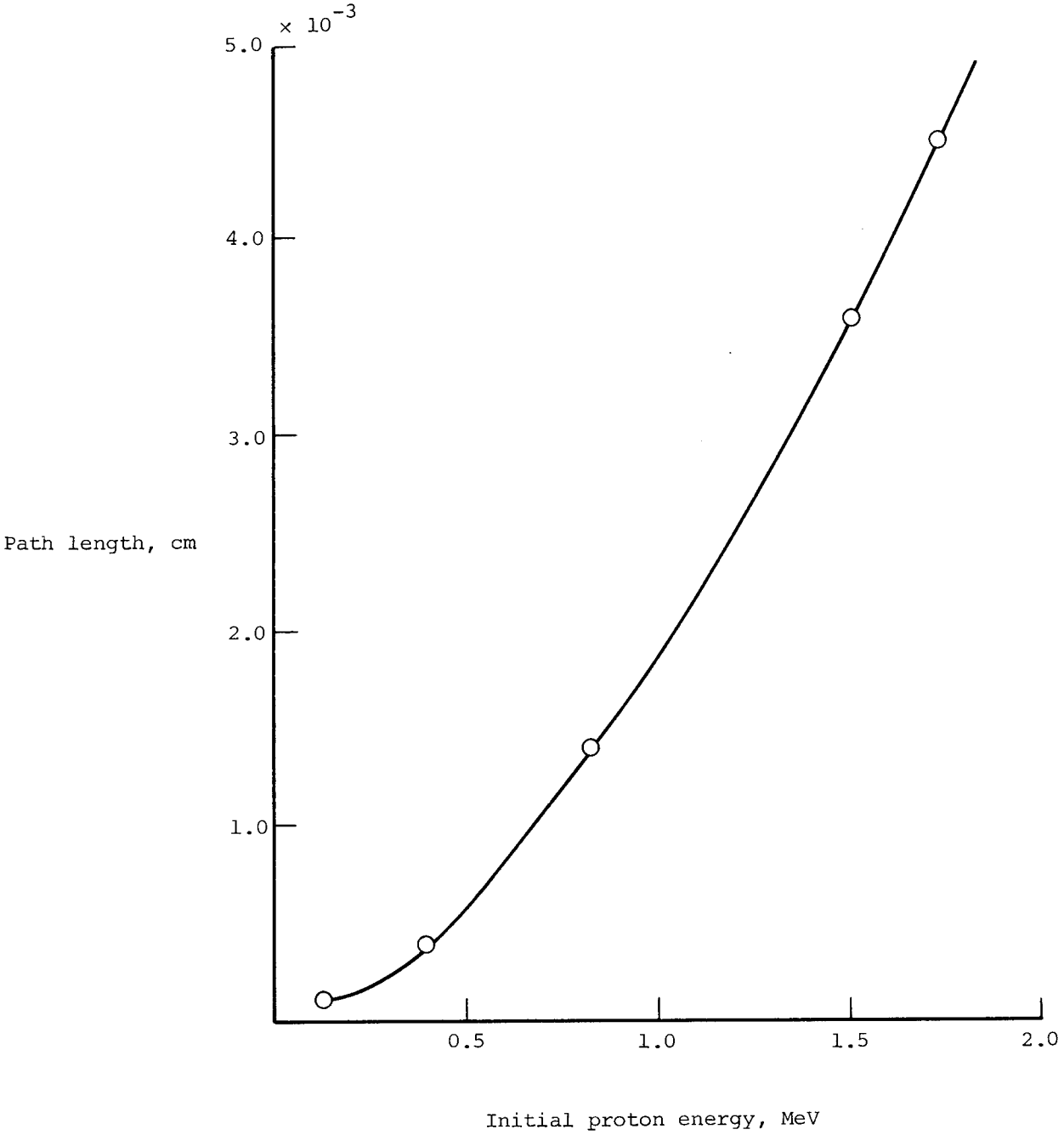

Figure 12.- Path length of protons in CNOSH1.

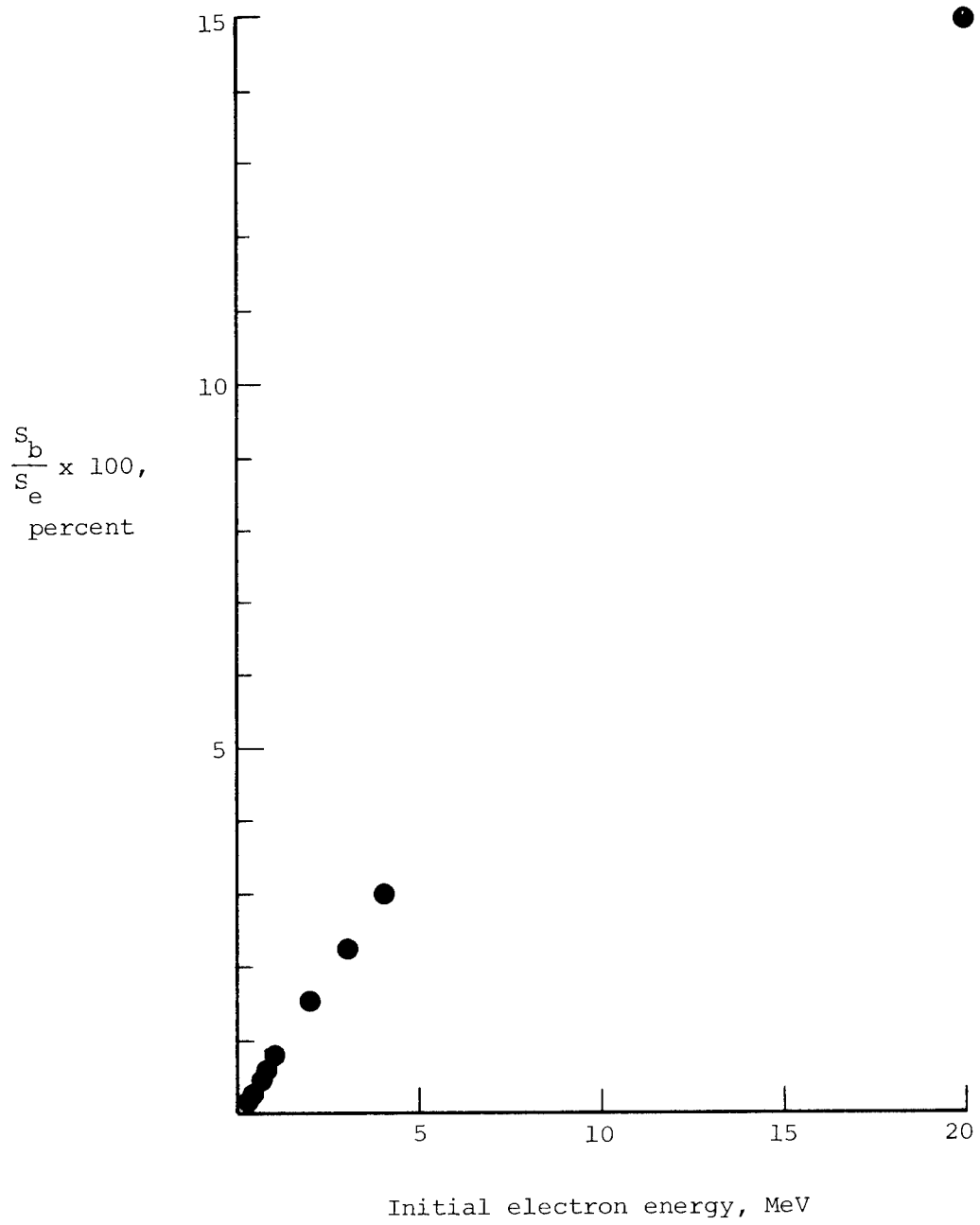

Figure 13.- Ratio of electron energy loss in CNOSH1 due to bremsstrahlung S_b, to energy loss due to inelastic scattering S_e.

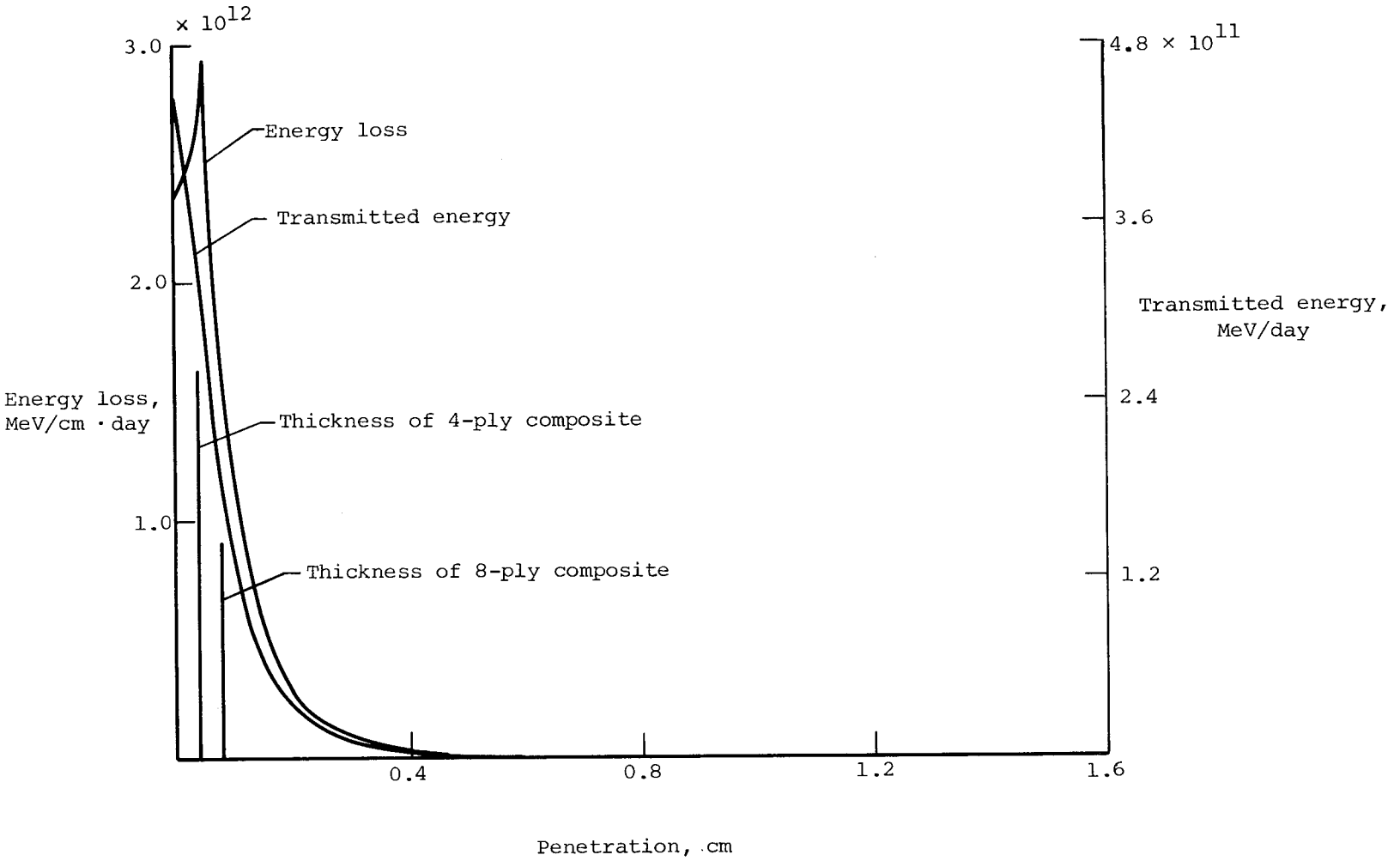

Figure 14.- Deposited and transmitted energy profiles in CNOSH1 for electron radiation in GEO.

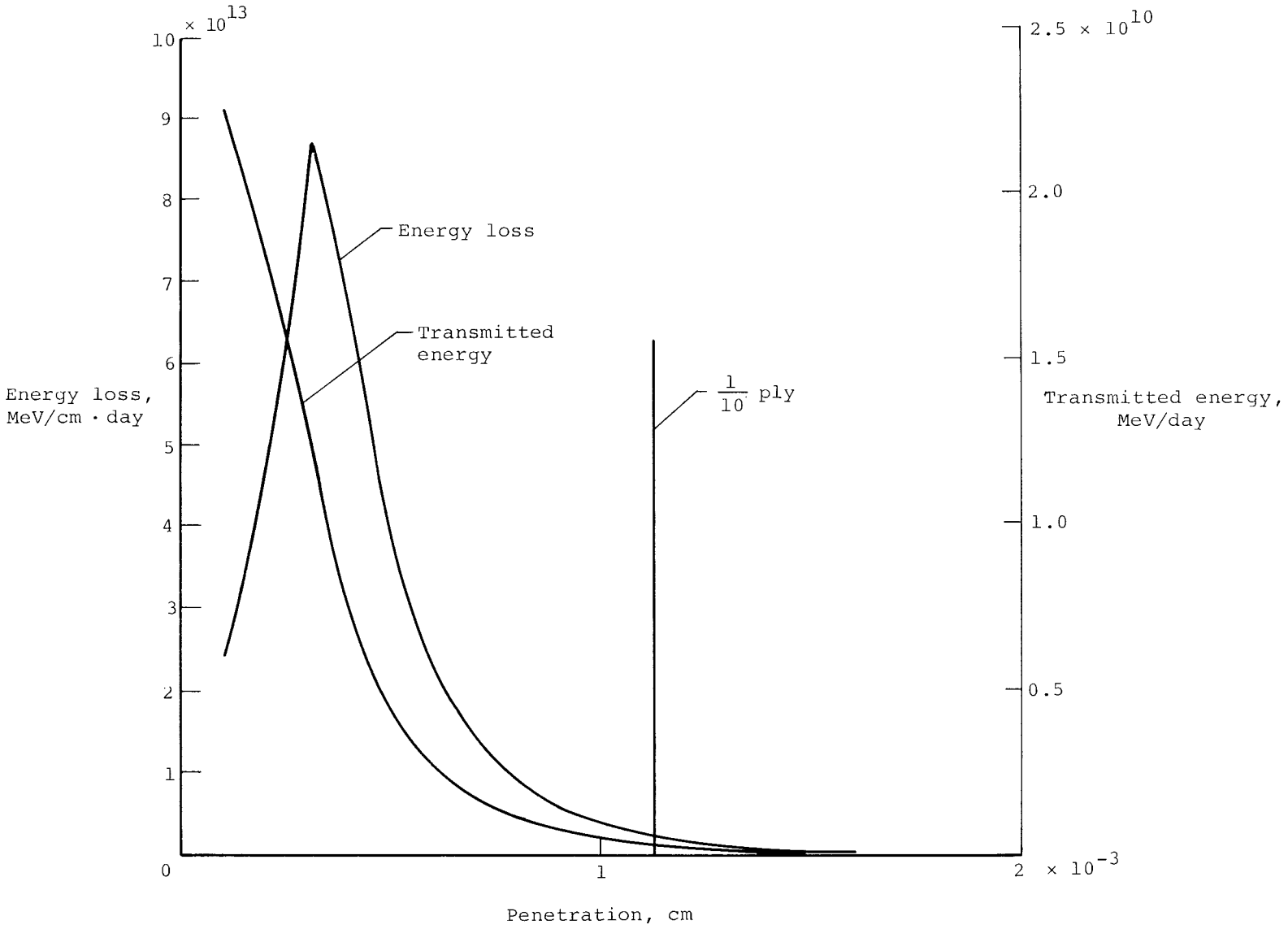

Figure 15.- Deposited and transmitted energy profiles in CNOSH1 for proton radiation in GEO.

1. Report No.	2. Government Accession No.	3. Recipient's Catalog No.
NASA TP-1568		

4. Title and Subtitle	5. Report Date
ELECTRON AND PROTON ABSORPTION CALCULATIONS FOR A GRAPHITE/EPOXY COMPOSITE MODEL	November 1979
	6. Performing Organization Code
7. Author(s)	8. Performing Organization Report No.
Edward R. Long, Jr.	L-13073
	10. Work Unit No.
	505-33-33-03
9. Performing Organization Name and Address	11. Contract or Grant No.
NASA Langley Research Center Hampton, VA 23665	
	13. Type of Report and Period Covered
12. Sponsoring Agency Name and Address	Technical Paper
National Aeronautics and Space Administration Washington, DC 20546	14. Sponsoring Agency Code

15. Supplementary Notes

16. Abstract

The Bethe-Bloch stopping power relations for inelastic collisions have been used to determine the absorption of electron and proton energy in cured neat epoxy resin and the absorption of electron energy in a graphite/epoxy composite. Absorption of electron energy due to bremsstrahlung has also been determined. Electron energies from 0.2 to 4.0 MeV and proton energies from 0.3 to 1.75 MeV were used in this study. Monoenergetic electron energy absorption profiles for models of pure graphite, cured neat epoxy resin, and graphite/epoxy composites are reported. A relation was determined for depth of uniform energy absorption in a composite as a function of fiber volume fraction and initial electron energy. Monoenergetic proton energy absorption profiles were reported for the neat resin model. A relation for total proton penetration in the epoxy resin as a function of initial proton energy was determined. Electron energy absorption in the composite due to bremsstrahlung was reported. Electron and proton energy absorption profiles in cured neat epoxy resin were also reported for environments approximating geosynchronous Earth orbit.

17. Key Words (Suggested by Author(s))	18. Distribution Statement
Graphite/epoxy composite Electron radiation Proton radiation Radiation absorption Dose-depth profiles	Unclassified - Unlimited Subject Category 27

19. Security Classif. (of this report)	20. Security Classif. (of this page)	21. No. of Pages	22. Price*
Unclassified	Unclassified	30	$4.50

* For sale by the National Technical Information Service, Springfield, Virginia 22161

NASA-Langley, 1979